ELSEVIER

Journal of Power Sources 84 (1999) 248–258

JOURNAL OF POWER SOURCES

www.elsevier.com/locate/jpowsour

High power metal hydride bipolar battery

K. Wiesener [a], D. Ohms [b,*], G. Benczúr-Ürmössy [c], M. Berthold [a], F. Haschka [c]

[a] *Kurt-Schwabe-Institut für Meß- und Sensortechnik e.V. Meinsberg, Ziegra-Knobelsdorf, Germany*
[b] *Accumulatorenwerke HOPPECKE, Carl Zoellner & Sohn GmbH & Co. KG, D-59929 Brilon, Bontkirchener Str. 2, Germany*
[c] *Deutsche Automobilgesellschaft, Esslingen, Germany*

Accepted 28 June 1999

Abstract

Nickel/metal hydride batteries in a bipolar design offer some advantages for an application as a power storage system for electric and hybrid vehicles. The paper deals with some aspects of combining a number of sub-cells in a common vessel design.

Keywords: Bipolar design; Nickel–metal hydride; Hybrid vehicle; Alkaline battery; Hydrogen absorption; Electrolytic creepage

1. Introduction

From the historic point of view a bipolar cell design (Volta's pile) belongs to the very first inventions in battery electrochemistry. The application of a bipolar cell design offers several advantages and therefore methods are sought to introduce the design principle in modern batteries. The design principle is strongly influenced by the choice of the electrochemical couple of the storage system. Deutsche Automobilgesellschaft (DAUG) and Kurt Schwabe Institut für Meß- und Sensortechnik e.V. Meinsberg (KSI) had joined to investigate this new type of battery. This project (1994–1998) was supported by the BMBF and it will be continued by a cooperation of Accumulatorenwerke HOPPECKE and KSI.

1.1. Bipolar cell design

The benefits of a bipolar cell technique in electrochemical engineering results in

– an easier construction principle and a smaller amount of passive materials
– lower handling and production costs
– a shorter electron path, resulting in lower internal resistance
– a higher specific power and specific energy
– a compact design for power sources with a high voltage.

An illustration of the stack is displayed in Fig. 1. The positive electrode of any cell unit (sub-cell) is directly electronically connected with the negative electrode of the next cell unit via a thin contact plate. The first and the last sub-cells are connected to the stack terminals.

The difficulties of a bipolar cell arrangement are

– the necessity of special precautions to avoid electrolytic short circuits between the sub-cells (e.g., via the bipolar contact plates)
– the sensitivity of the bipolar contact plates on their positive side against corrosion reactions (electric resistance)

1.2. Nickel–metal hydride system

In comparison to other advanced battery systems the nickel/metal hydride-battery system offers high specific energy and power and is working with an aqueous electrolyte at ambient temperatures. The Ni/MH couple is based on a rather simple ion transfer reaction similar to the lithium ion shuttle system (Fig. 2). As this will not include the electrolyte in the overall cell reaction this offers the opportunity to realize a bipolar design for battery stacks with a limited amount of starved electrolyte.

Thus, sealed Ni/MH batteries in bipolar cell design are of special interest for an application as energy storage in hybrid road vehicles, since increasing specific power (less

* Corresponding author. E-mail: hoppeche.gtg.ohms@t-online.de

0378-7753/99/$ - see front matter
PII: S0378-7753(99)00325-0

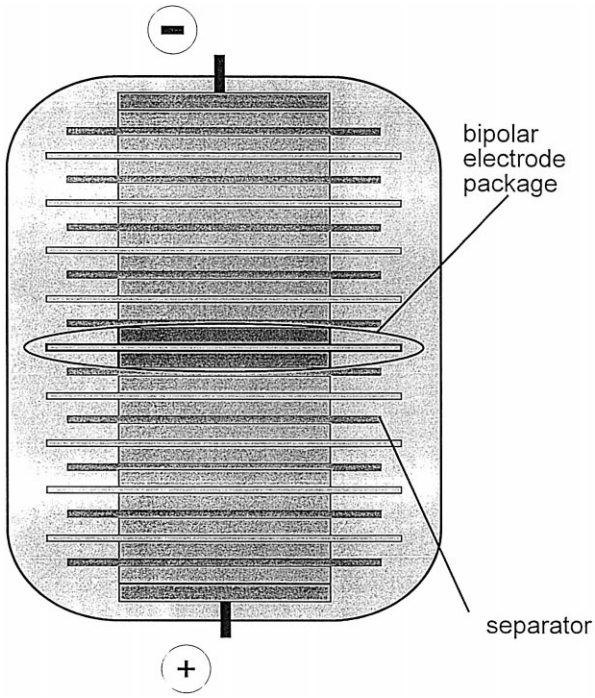

Fig. 1. Schema of a bipolar Ni/MH stack (12 V).

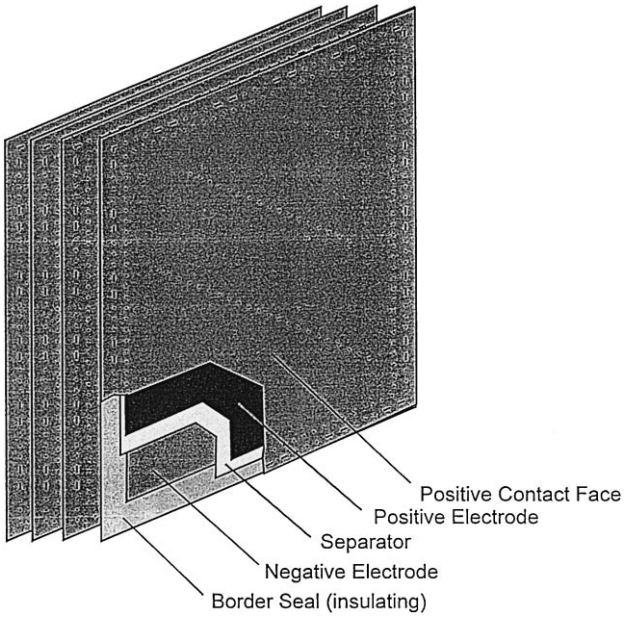

Fig. 3. Wafer cell concept according to Klein and Reisner (Electro Energy, Danbury).

cell containment), lower cost, easier handling (higher voltage packages) and better balance between individual sub-cells in comparison to series of conventional cells can be expected.

Ni–MH-Batteries in different bipolar cell designs have been under discussion for a couple of years [1–4,7]. For example, Klein [3] and Reisner et al. [4] used in their bipolar Ni/MH-cell arrangements so-called ''wafers'' consisting of a nickel- and a metal-hydride electrode with a separator between them and with contact sheets on both sides consisting of conductive carbon-filled plastic material (Fig. 3). The wafers have been enclosed by insulating peripheral heat sealing. The multi-cell batteries are assembled by stacking wafer cells under an external force.

2. Experimental

In our laboratory investigations all cell elements were stacked upon each other and are fixed in a tube (common-vessel). By applying mechanical pressure to the end plates, the sub-cells were electrically connected by a thin nickel plate and the separator, a non-woven polymer fibre material was soaked with the electrolyte before stacking. (Fig. 4).

In most of the laboratory bipolar stacks — containing 5 to 10 sub-cells — all bipolar plates were connected with an external recording device in order to measure voltage and resistance of any sub-cell of the bipolar stack during the experiments.

As the sub-cells are placed in a common vessel design they are inter-connected via the gas-phase. Thus, water vapour and reaction gases may be transferred between the sub-cells. For thermodynamical reasons a possible diverging of the negative electrodes in respect of their hydrogen content and temperature as well as the electrolytic concentration may be prevented.

In order to avoid the difficulties involved in a bipolar Ni/MH-cell arrangement, the following problems have to be solved:

– Providing of an adequate amount of electrolyte in all sub cells

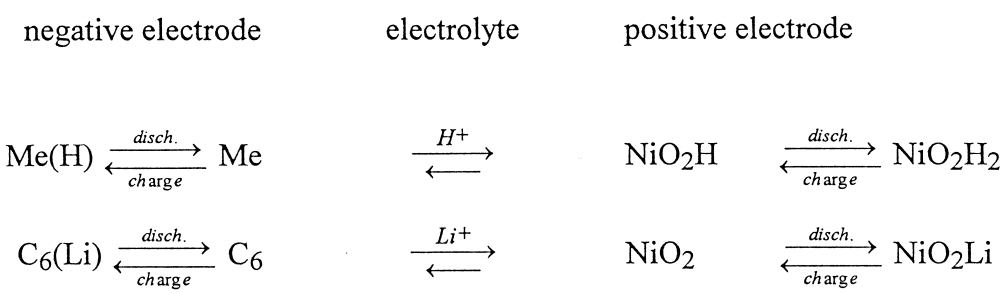

Fig. 2. Reaction schemes of ion shuttle systems.

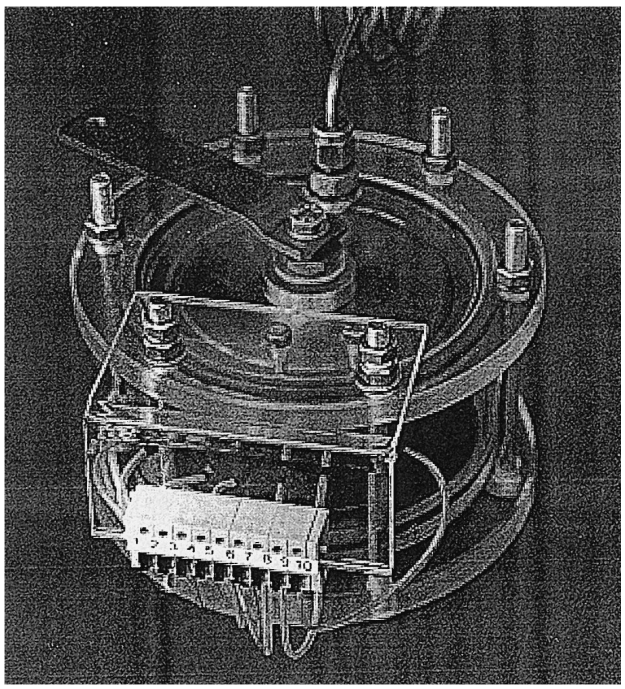

Fig. 4. Bipolar Ni/MH-stack (10 sub-cells) with electric connections to each bipolar plate.

- prevention of a non-uniform electrolyte distribution, prohibiting electrolytic creeping (electric resistance and self discharge)

– Providing an optimum contact force and optimum gas pressure

- minimizing of contact resistance

– Optimizing electrode thickness

– Providing a heat exchange to the surrounding

As is known from most alkaline cells electrolytic creepage is a serious problem especially at the negative ta. The electrolyte distribution in the bipolar cell stack has to be to controlled very exactly. A movement of electrolyte between the cell units results not only in a bypass current but also in an increase of the cell resistance by electrolyte pauperization in some cell units.

The formation of passive layers with low electronic conductivity on the bipolar back-plates has to be prevented by a suitable covering material.

3. Results

3.1. Electrical measurements

The electrochemical behaviour of the stacks has been studied in several experiments including cycling and pulse discharging. In Fig. 5, discharge curves of a bipolar stack (five sub-cells) with different currents are displayed and demonstrate the low internal resistance of the battery.

Further information on the resistance and polarisation behaviour has been obtained from pulse discharge measurements of a five-cell 2.5 A h stack (10 s pulse of 4 C, 60 s break), Fig. 6.

From the voltage drop recorded after applying the pulse current for 1 s, a resistance of 240 mΩ A h for a bipolar stack of five sub-cells has been computed. This results in an average of 48 mΩ A h per sub-cell. The resistance depends strongly upon the thickness of the electrodes used. Fig. 6 shows the behaviour of a stack with rather thick electrodes in contrast to Fig. 5. This resistance includes

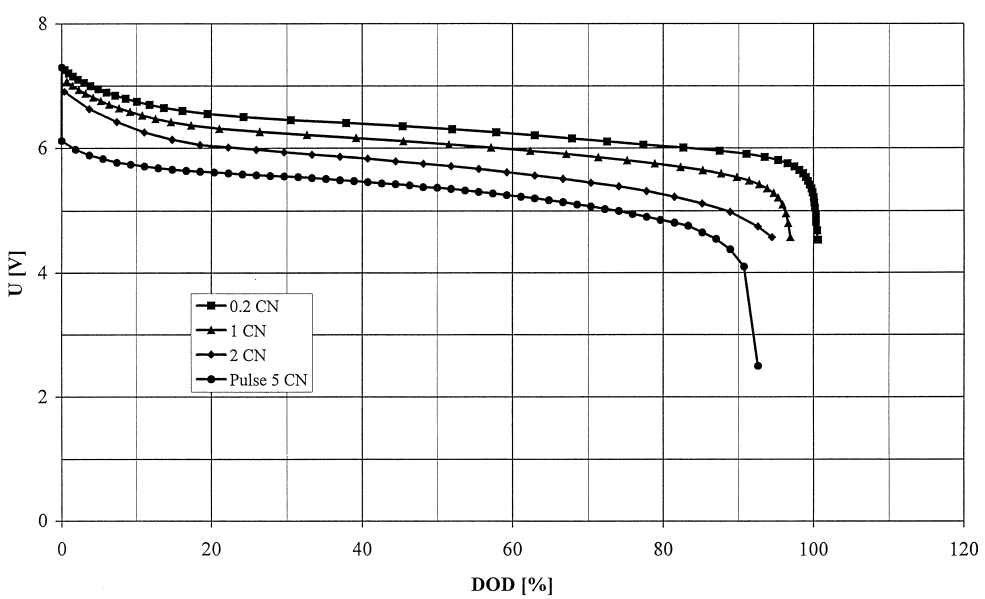

Fig. 5. Discharge curves of a bipolar Ni/MH stack (five sub-cells).

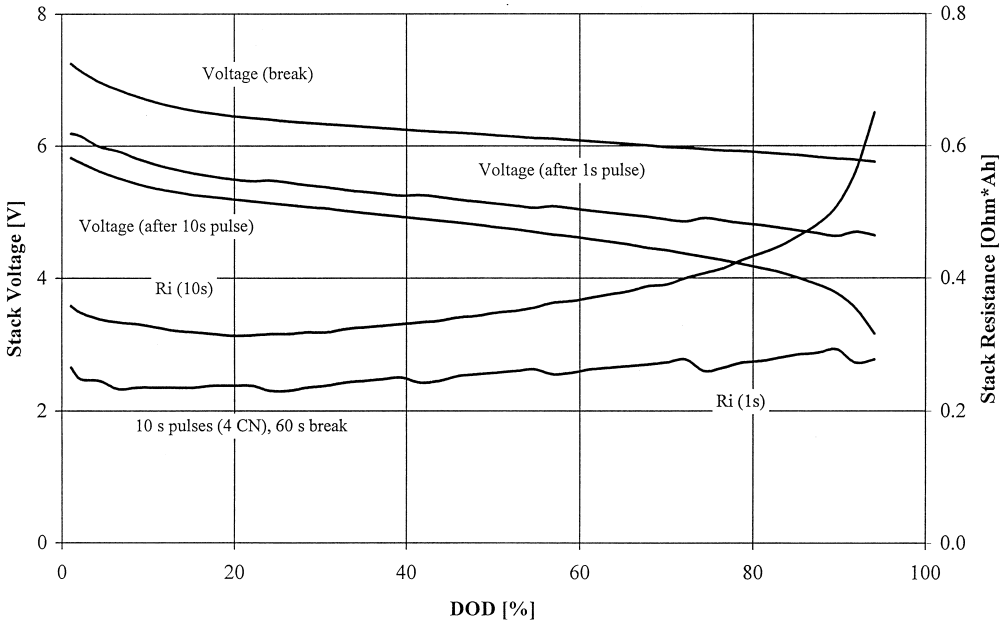

Fig. 6. Pulse discharge of a bipolar Ni/MH stack (five sub-cells, CN 2.5 A h).

ohmic drops as well as electrochemical polarisation. The computed resistance from the voltage drop 10 s after applying the pulse delivers higher values indicating an increasing cell polarisation with time.

In particular, at the end of discharge (80–90% DOD) the polarisation increases whereas the value measured after 1 s — involving mostly ohmic drops — remains low. Thus, at high DOD electrode kinetics and transport kinetics will affect the discharge process.

The stacks have performed several hundreds of deep discharge cycles. If parasitic currents are prevented (stacks C–F) self-discharge is as low as in monopolar arrangements (stack A or conventional cells) (Fig. 7). In case of insufficient electrolytic separation (stack B) the self discharge is large.

3.2. Hydrogen exchange between sub-cells

The thermodynamics and kinetics of the exchange of hydrogen between the sub-cells were studied as this will

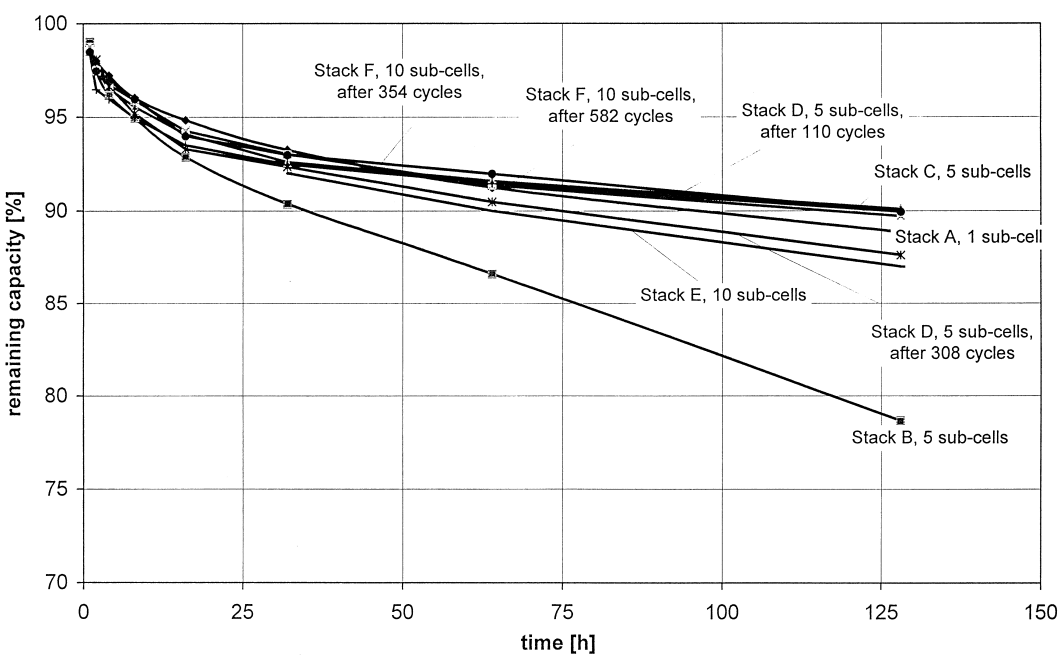

Fig. 7. Self-discharge behaviour of different bipolar Ni/MH-laboratory stacks.

influence the functioning of the complete stack. There is a thermodynamic relationship between state of charge of the negative electrodes, the temperature and the hydrogen pressure [7]. During most of the operation time the cell pressure remains low (<1 bar). Only at the high SOC (state of charge), e.g., $>80\%$, and elevated temperatures ($>50°C$) does the pressure become higher than the surrounding. Therefore, hydrogen may be exchanged if temperature or SOC of adjacent sub-cells differ. In order to study the hydrogen exchange between the sub-cells in a bipolar stack the following experiments have been carried out.

For this investigations, the situation in a bipolar stack was simulated by using two conventional cells containing similar electrodes. The cells were connected via a separate gas vessel of known volume and placed in water bath of constant temperature or kept adiabatically (Fig. 8).

At the beginning of the experiments the cells were charged to a given SOC. Two different measuring procedures were used. Firstly (method 1), the volume of hydrogen exchanged was measured by stepwisely transferring portions of the gas from one cell to the other via a known volume of the connecting tubes (sequentially opening and closing of the valves of the connecting tubes between the two cells). Secondly (method 2), we calculated the transferred hydrogen amount from the heat of absorption (36.4 $kJ/mol\ H_2$) and the heat capacity of the cell by measuring the temperature rise of the hydrogen-receiving cell, which was thermally isolated. The calculated values of the hydrogen transfer obtained by the two different methods described above were in satisfactory agreement.

For cells with different SOC (10–30%) but the same starting temperature, the hydrogen amount transferred during a given time and related to the theoretical value (computed from the SOC difference) is mainly proportional to the pressure difference between the two cells (Fig. 9).

Considering the same SOC difference between the cells, the hydrogen pressure difference and the exchange rate become larger at higher levels of SOC. Thus, the rate of the hydrogen transfer in the case of small pressure differences (<50 mbar) is very slow.

Secondly, the hydrogen loading of the negative electrode does not necessarily correspond to the SOC of the cells as the latter is determined by the positive electrodes. In order to overcome these experimental difficulties, the cells were charged to the same SOC and the gas-filled parts were connected for 12–24 h across the connecting tube before the experiments were started. This should level the hydrogen loading of the negative electrodes.

The transferred amount of hydrogen of cells with a cell temperature difference of 10 K and the same SOC was ~ 60 mmol which corresponds to about 4% of the nominal $A \cdot h$-capacity of the cell. Sixty millimoles of hydrogen will deliver or consume approximately 2.16 kJ in absorption or desorption, respectively. Taking into account the heat capacity, the temperature of the hydrogen absorbing cell was raised by about 1 K, and the temperature of the hydrogen delivering cell was reduced by 1 K (adiabatic conditions). Thus, the temperature difference of the cells decreases from 10 K to 8 K.

In order to get further information on the kinetics of the gas transfer, the sorption process was investigated in two different relaxation experiments with smaller amounts of hydrogen than in the experiments described above (Fig. 10).

Before the experiment an equilibrium state was established. Adding a small portion of hydrogen will disturb this equilibrium state and leads to a new equilibrium state. Assuming a first order reaction for absorbing the hydrogen

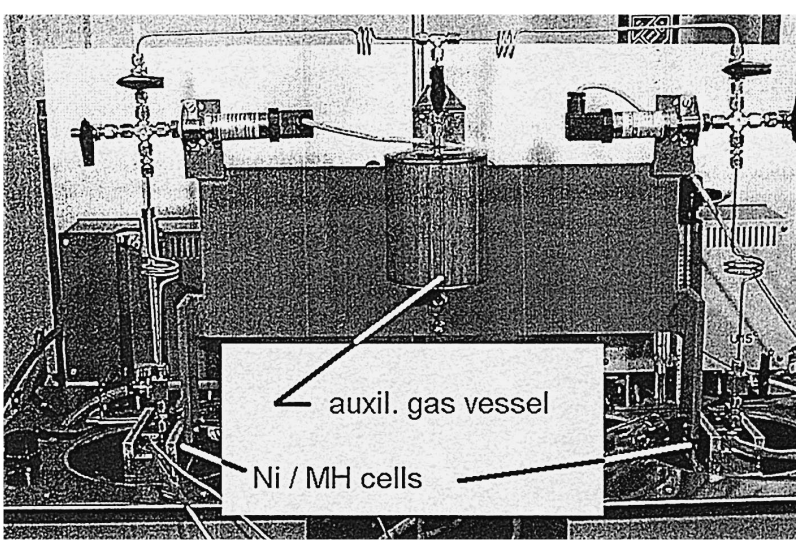

Fig. 8. Measuring device for the investigation of the hydrogen exchange.

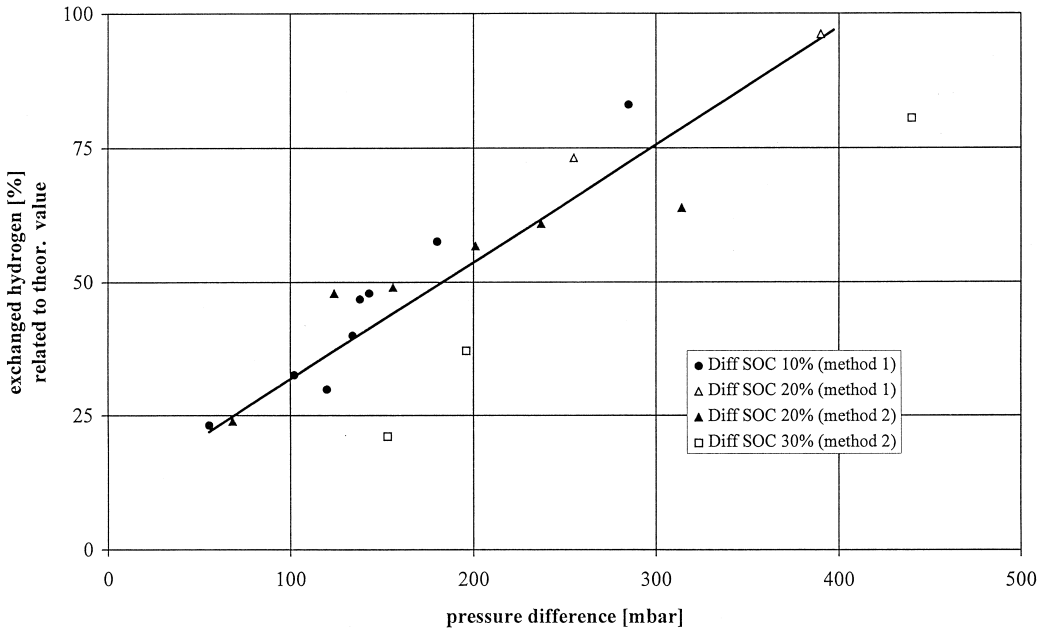

Fig. 9. Hydrogen transfer at 25°C during 4 h between two Ni/MH cells of variable SOC differences and different experimental methods.

the half-life time of the reaction can be determined. After establishing the new equilibrium the evacuated tubes are connected to the cell. Thus, a small portion of gas is released from the metal hydride and again the half-life time of the desorption may be obtained. The result of the relaxation experiment is given in Fig. 10. The relaxation times for both absorption and desorption are about 190 s.

The higher velocity of the gas absorption and desorption in comparison to the previous experiments may be explained by the limited amount of hydrogen in the relaxation experiment. Obviously the absorption and desorption of a small amount of hydrogen is restricted to the surface of the metal hydride. The exchange of huge amounts involves also the bulk transport of hydrogen in the grains.

3.3. Electrolyte creepage

In our first investigations on bipolar arrangements we observed an increase of the internal resistance of the cell stack during cycling. In order to find an explanation for that finding we studied the data of the individual sub-cells during the charge/discharge cycles and pulse experiments (Fig. 4). In a five-sub-cell stack the voltage and the resistance of four of the five sub-cells behaved very simi-

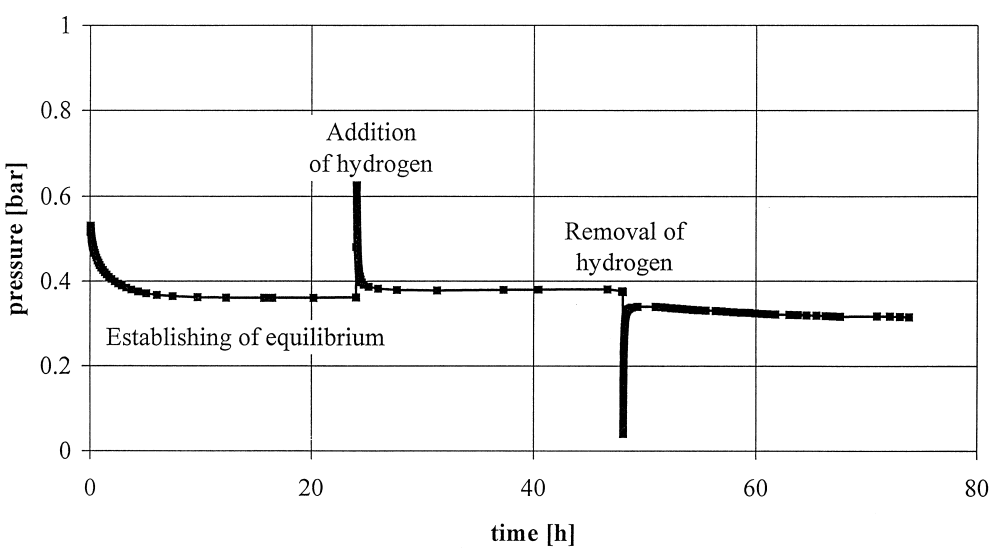

Fig. 10. Relaxation experiments of hydrogen reaction in a Ni/MH cell at 25°C.

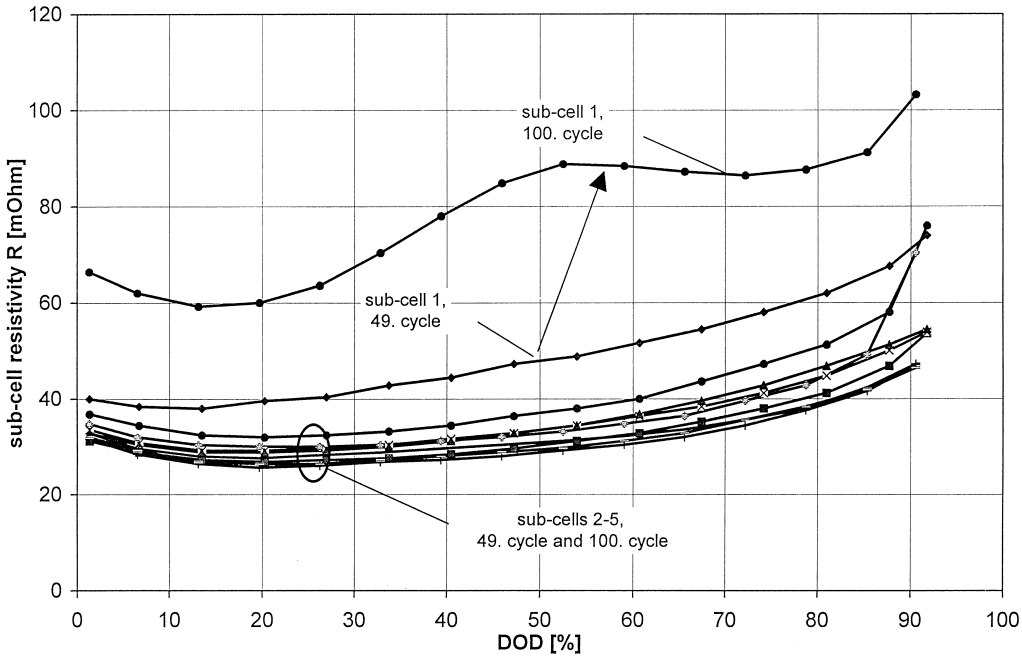

Fig. 11. Change of resistance of sub-cells in a bipolar stack 4 C (10 s pulses) with increasing cycle numbers.

larly during the cycling and pulse discharge. The sub-cell (sub-cell 1) at the positive terminal of the stack showed a different behaviour (Fig. 11). Its resistance was increasing during the cycling to a value considerably higher than that of the other sub-cells.

As all cells were prepared in the same manner this difference was unexpected. The reason was found by investigating the electrolyte distribution after disassembling the stack. (Fig. 12).

According to the distribution after cycling the effect observed can be attributed to an unbalancing of the amounts of electrolyte. The loss of absorbed electrolyte from the separator (electrolyte carrier) leads to an increase of the resistance of the sub-cell and of the whole battery stack. This underlines the role of measures to prevent any electrolyte creepage in bipolar arrangements.

The disturbance of the electrolyte balance cannot only be attributed to capillary forces and different wettability of

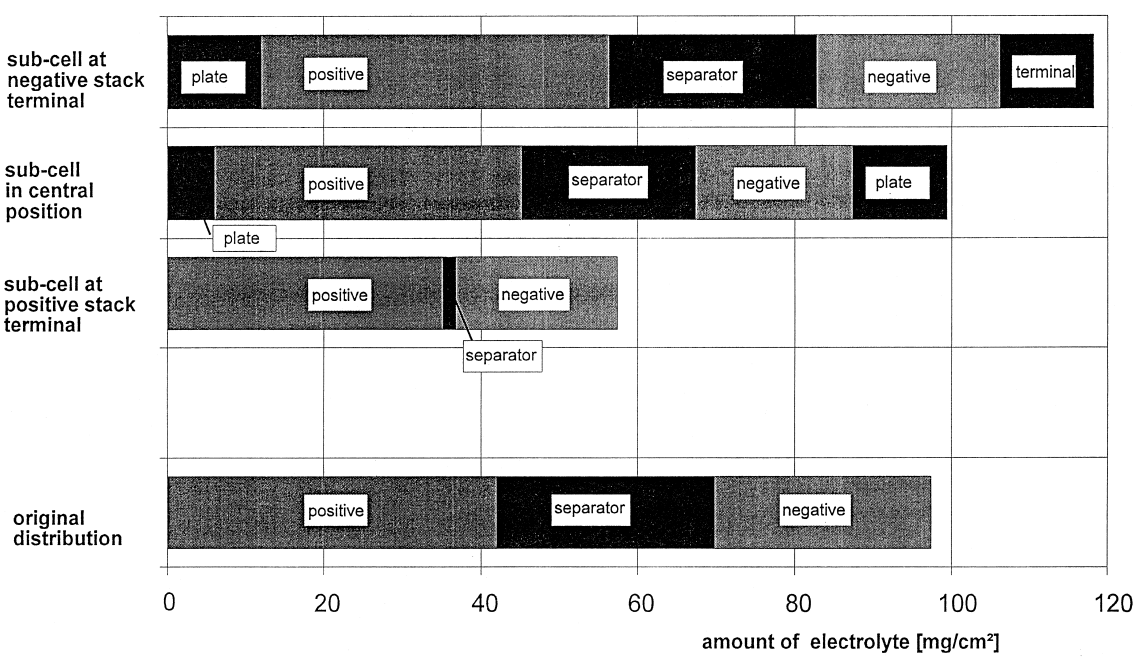

Fig. 12. Distribution of the electrolyte in the sub-cells before and after cycling.

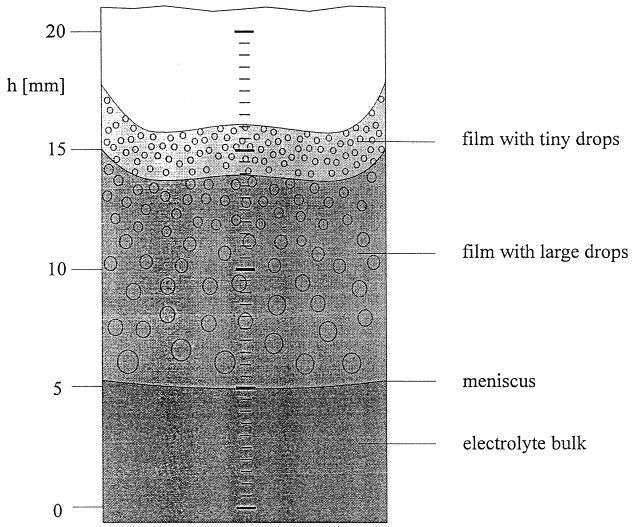

Fig. 13. Creepage of electrolyte on an immersed Ni-plate.

the materials used. In addition, the electric potential plays a major role in the electrolyte transfer.

The electrolytic creepage of alkaline electrolytes at metal surfaces forced by the electric field has been already described in the 1970s by Hull and James [5] and Davis and Hull [6]. We studied this problem using a special experimental set-up. A nickel plate was partially immersed in the electrolyte (Fig. 13).

Using a nickel counter electrode and a Hg/HgO reference electrode we applied a potential of $E = -900$ mV (vs. Hg/HgO) close to that at the negative electrode during the charging process. Air or nitrogen pre-saturated with moisture was present above the electrolyte. During the experiment in the presence of air the electrolyte wets the nickel plate, starting with deposition of tiny drops above the meniscus developing via large condensate drops to a complete creepage film on the surface (Fig. 14).

The creepage height increases with time. In the absence of oxygen no creepage will be observed during the polarisation of the nickel plate. Therefore, the assumption is made that the surface of the nickel is wetted by an electrolytic attack in an electrochemical mechanism. In this mechanism the oxygen is reduced at the most negative spots of the surface as illustrated in Fig. 15.

The creepage is related to an increase of the amount of electrolyte at the edges of the wetted zone. The volume of electrolyte in zone B may be raised by a transport of water via the vapour phase. This is initiated by a difference in the partial pressure of water vapour above different zones of the plate. Such points of different vapour pressure are caused by variations of electrolytic (OH^-) concentration.

At the applied electrode potential in the presence of oxygen — formed during the overcharge reaction of the positive electrode — an increase of the OH^- ion concentration in the reaction zone B should take place. The electrolyte covering will not hinder the oxygen reaching the surface and the oxygen reduction can take place very fast. This explains why, in the absence of oxygen, the creepage will not take place. This leads to further covering of the nickel plate on the negative side with electrolyte and, finally, the electrolyte is shifted from the negative side of the contact plate between the sub-cells to the positive side of the next sub-cell. This process takes place

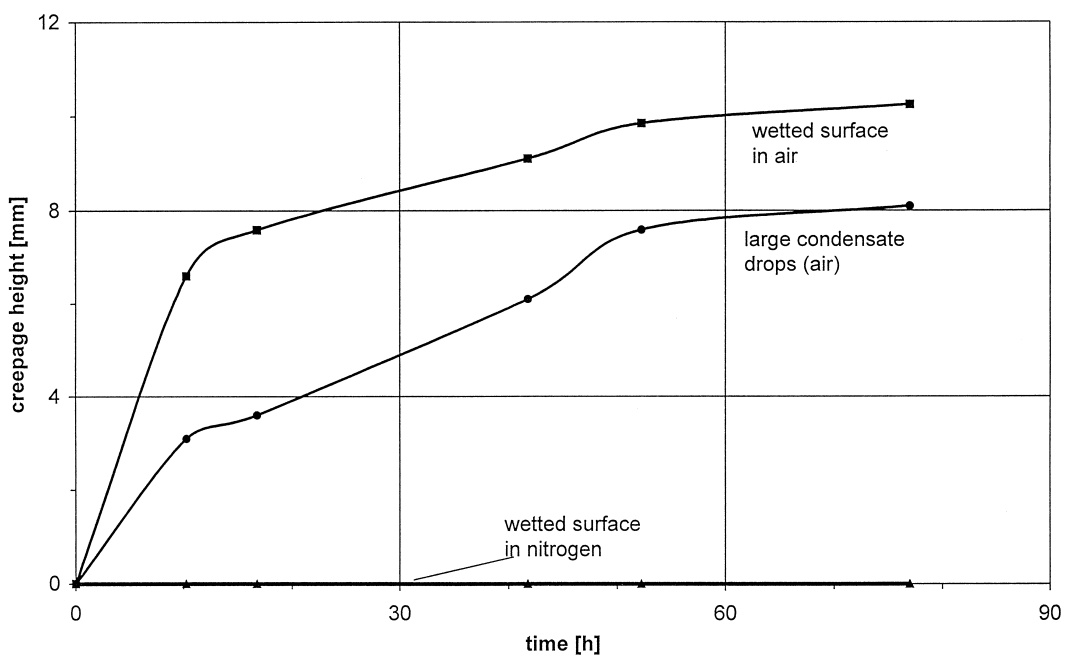

Fig. 14. Creepage height as function of time on a Ni-plate immersed in the electrolyte at $E = -0.9$ V vs. Hg/HgO under different gases.

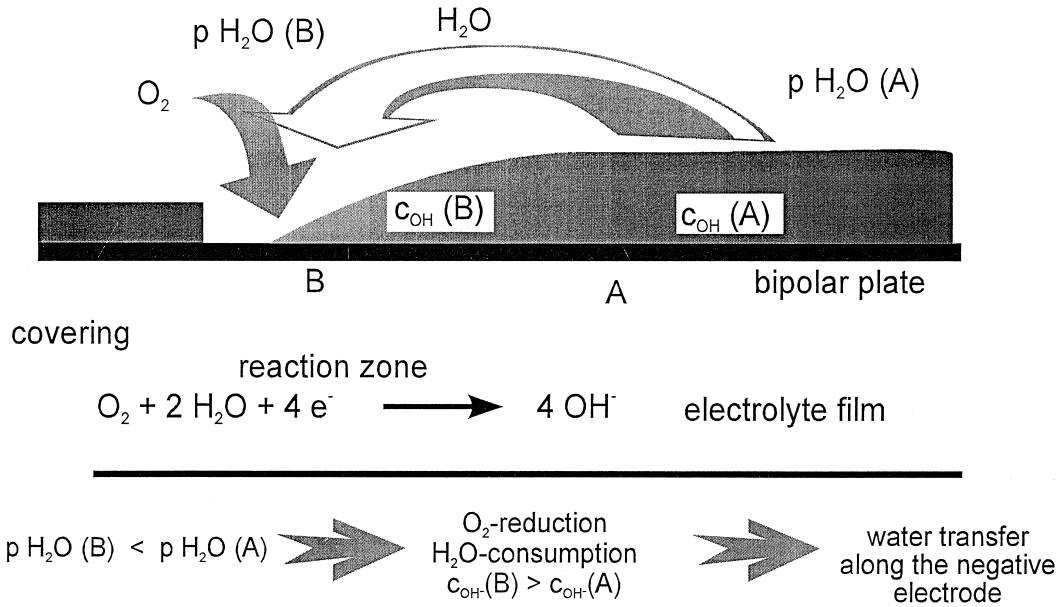

Fig. 15. Formation of a creepage film on a Ni-plate.

even if the electrolytic transfer occurs against the gravitational force.

Taking into account this effect we tried to prevent the electrolyte creepage by covering the metallic surface. As a result, the electrolyte distribution was not changed during the experiments (even after 255 cycles) as demonstrated in Fig. 16.

3.4. Tests for hybrid vehicle application

Hybrid vehicles need power storage devices with large power/energy ratios. The battery has to be able to deliver and to absorb energy in short pulses. In addition, the charging efficiency should be known at different SOC. For such an application we have performed experiments with a bipolar 10-cell stack. The results are compiled in Table 1.

As a first result charge and energy efficiency (but to a minor extent) rise with decreasing initial SOC. Applying a charging factor of 1.025 the SOC remains constant when the initial SOC of the cycle test is about 60% of the nominal capacity. In the case of a lower value (40% of the nominal capacity) the charge state increases and, at a higher initial SOC (80% of the nominal capacity), the

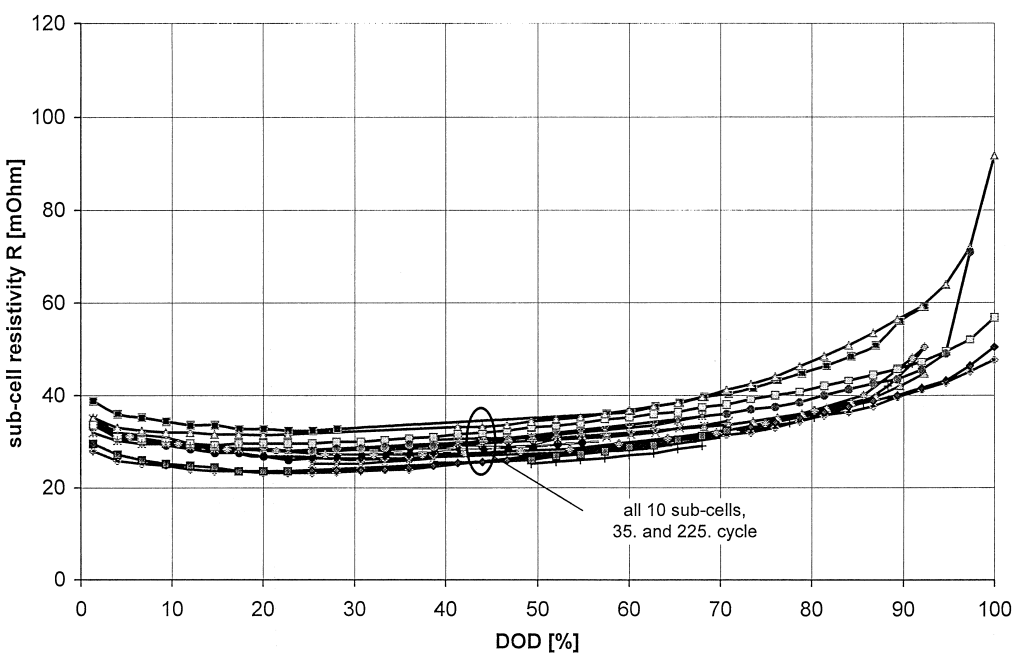

Fig. 16. Resistance of sub-cells in a bipolar stack 4 C (10 s pulses) with increasing cycle numbers of a bipolar cell stack of the second generation.

Table 1
Charge- and energy efficiency of a bipolar Ni/MH stack (10 sub-cells) during cycling with high currents at different starting SOC

Rated capacity	2 A h
Number of cycles	50
Charge and discharge current	10 A (5 C)
DOD per cycle	0.2 A h (10% of rated capacity)
Charge factor	1.028
Discharge time	72 s
Charge time	74 s
Break between charge and discharge	144 s

Initial charging state (A h)	Initial charging state (% SOC)	Remaining capacity after 50 cycles (A h)	Mean discharge voltage (V)	Mean charging voltage (V)	A h-efficiency (%)	Energy efficiency (%)
1.60	80	1.49	11.43	15.16	97.0	73.1
1.20	60	1.25	11.34	15.09	98.7	73.8
0.80	40	1.00	11.16	14.96	99.6	74.3

charging factor is too low to maintain the SOC during cycling at the starting level. This means that self-discharge and parasitic side reactions during the charge process decrease with the SOC of the battery. From this point of view it seems advisable to use in general a SOC between 50 and 65%, where the battery on one hand should have enough storage capacity for a peak power demand and additionally is able to absorb the braking energy of the hybrid vehicle with high efficiency.

Cycling with bipolar cells has been continued for more than 1000 charge/discharge cycles without any failures. In Fig. 17, an example is shown with different load factors and starting DOD. The cycling behaviour of the stack is very stable; voltage and pressure are changing between the same limits during a long period of time.

4. Conclusion

The results of the experiments have shown that a nickel/metal hydride battery in bipolar design is a realistic alternative for the power storage device in a hybrid vehicle. After solving the principal problems in the small cells, we succeeded in constructing a 50 V (2 kW maximum power) laboratory stack (39 sub-cells), with a capacity of

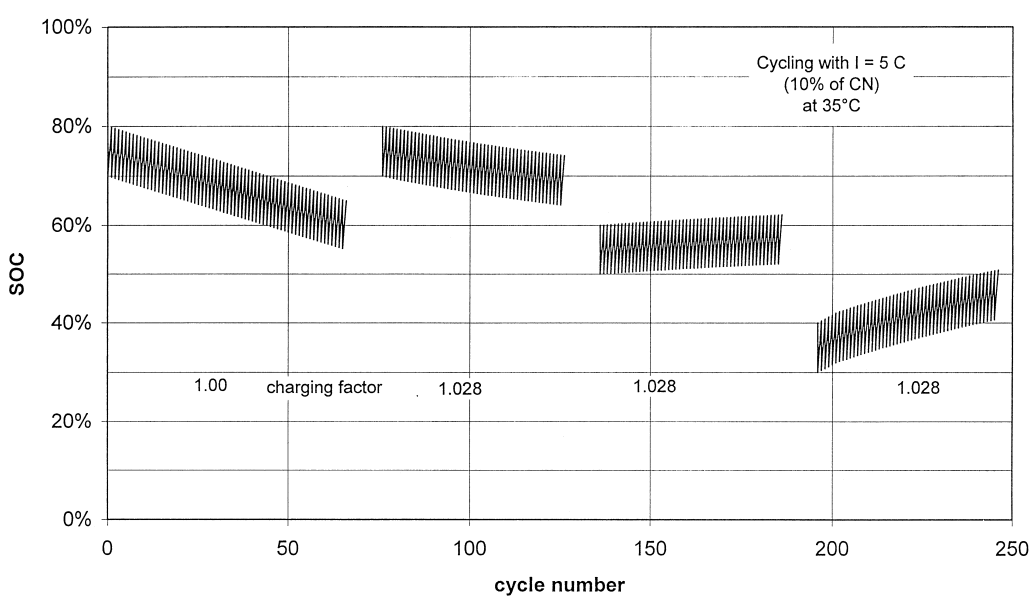

Fig. 17. Cycle test of a bipolar Ni/MH-stack of 10 sub-cells with different load and DOD.

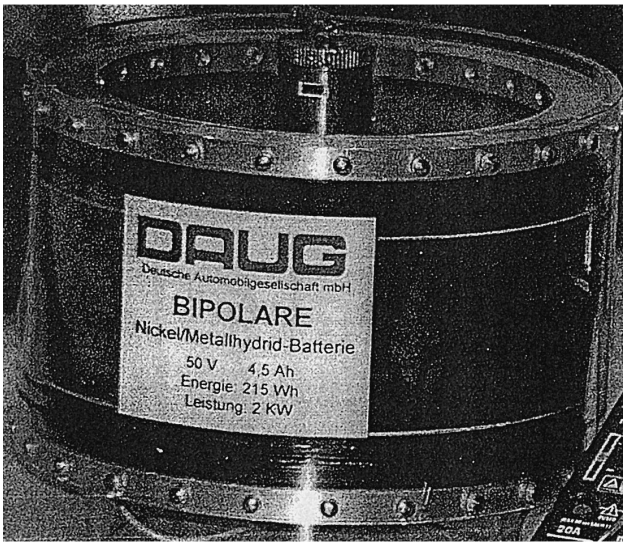

Fig. 18. Bipolar 50 V–2 kW-Ni/MeH-laboratory stack, capacity: 4.5 A h; energy: 215 W h.

4.5 A h or 215 W h, respectively (Fig. 18). The stack was tested and it demonstrated the high power capability of the system and the expected good cycling behaviour.

It has been shown that the bipolar cell design is an interesting alternative design for Ni/MH cells. Immobilizing and stabilizing the electrolyte in the separate sub-cells and preventing its creepage are the key problems to be solved. In our opinion, the bipolar Ni/MeH-battery seems to be the system of choice for an application in hybrid vehicles in combination with combustion engines. By the use of thin electrodes power densities upto 1 kW/kg may be realized. In addition, it is also of advantage to use such a battery in vehicles with fuel cell generators. The reasons for that are:

– Reduction of the dynamic power demand for the fuel cell
– Peak power is less expensively realized by alkaline Ni/MH-batteries than by fuel cells (ca. US$50/kW)
– Minimizing the volume requirements of the complete system (reforming unit, auxiliary systems, fuel cell stack)
– Utilization of regenerative broking energy
– High power supply to start before main power system is switched to full performance
– Improved characteristics at low temperatures (< 0°C)
– Independent power storage system (esp. for direct methanol fuel cells)

Acknowledgements

The authors acknowledge the BMBF (Bundesministerium für Bildung, Wissenschaft, Forschung und Technologie) (project BEO 0329621 A/B) for financial support of the research activities and Dr. G. Sandstede for helpful discussion.

References

[1] D. Ohms, G. Benczúr-Ürmössy, F. Haschka, W. Warthmann, Proc. EVT'95, Paris, Nov. 11–13, 1995.
[2] W. Warthmann, G. Benczúr-Ürmössy, F. Haschka, D. Ohms, Proc. 13th Int. Sem. Primary and Secondary Batt. Tech. Eng. Appl., Boca Raton, March 4–7, 1996.
[3] M. Klein, US Pat. 5,393,617, issued Feb. 28, 1995.
[4] D.E. Reisner, J.H. Cole, M. Klein, Proc. EVS-13, Osaka, Oct. 13–16, 1996.
[5] M.N. Hull, H.I. James, J. Electrochem. Soc. 124 (1977) 332.
[6] S.M. Davis, M.N. Hull, J. Electrochem. Soc. 125 (1978) 1918.
[7] G. Benczúr-Ürmössy, F. Haschka, D. Ohms, K. Wiesener, M. Berthold, Jahrestagung der Fachgruppe der GDCh, Angewandte Elektrochemie, Elektrochemische Verfahrenstechnik - Energietechnik, Stoffgewinnung, Bioelektrochemie, 9.12.10.1996, Monheim, GDCh-Monographie, 9, GDCh, Frankfurt, 1997, pp. 161–162.